Ice-stream initiation, duration and thinning on James Ross Island, northern Antarctic Peninsula

This is a pre-print version of a paper that is published in *Quaternary Science Reviews.* Please visit and cite the online version of the paper. The full reference is:

Glasser, N.F., B.J. Davies, J.L. Carrivick, A. Ròdes, M.J. Hambrey, J.L. Smellie and E. Domack (2014). Ice-stream initiation, duration and thinning on James Ross Island, northern Antarctic Peninsula. *Quaternary Science Reviews* **86**, 78-88.

Link: http://www.sciencedirect.com/science/article/pii/S0277379113004551

N.F. Glasser[1†], B.J. Davies[1], J.L. Carrivick[2], A. Rodes[3], M.J. Hambrey[1], J.L. Smellie[4], E. Domack[5]

[1]Department of Geography and Earth Sciences, Aberystwyth University, Wales, SY23 3DB, UK.
[2]School of Geography, University of Leeds, LS2 9JT, UK
[3]SUERC, East Kilbride, UK
[4]Department of Geology, University of Leicester, University Road, Leicester LE1 7RH, UK
[5]Department of Geosciences, Hamilton College, Clinton, New York 13323, USA
†Email: nfg@aber.ac.uk

ABSTRACT

Predicting the future response of the Antarctic Ice Sheet to climate change requires an understanding of the ice streams that dominate its dynamics. Here we use cosmogenic isotope exposure-age dating (^{26}Al, ^{10}Be and ^{36}Cl) of erratic boulders on ice-free land on James Ross Island, north-eastern Antarctic Peninsula, to define the evolution of Last Glacial Maximum (LGM) ice in the adjacent Prince Gustav Channel. These data include ice-sheet extent, thickness and dynamical behaviour. Prior to ~18 ka, the LGM Antarctic Peninsula Ice Sheet extended to the continental shelf-edge and transported erratic boulders onto high-elevation mesas on James Ross Island. After ~18 ka there was a period of rapid ice-sheet surface-lowering, coincident with the initiation of the Prince Gustav Ice Stream. This timing coincided with rapid increases in atmospheric temperature and eustatic sea-level rise around the Antarctic Peninsula. Collectively, these data provide evidence for a transition from a thick, cold-based LGM Antarctic Peninsula Ice Sheet to a thinner, partially warm-based ice sheet during deglaciation.

INTRODUCTION

The Antarctic Peninsula is one of the most rapidly warming areas of the Earth (Turner et al., 2005, Vaughan et al. 2003), with warming and snow-melt rapidly accelerating over the last century (Abram et al., 2013), increases in precipitation (Turner et al., 2009), a longer melt season (Barrand et al., 2013) and enhanced moss growth and microbial activity (Royles et al., 2013). The north-eastern Antarctic Peninsula is sensitive to even small changes in atmospheric temperature, with glacier acceleration, thinning and recession, and the collapse of several large ice shelves observed in recent decades (Cook et al. 2005, 2010; Pritchard et al., 2012).

Documented changes in Antarctica also include the rapid and dynamic fluctuations of the Siple Coast ice streams (Joughin et al. 2002) and the recent recession, acceleration and thinning of Pine Island Glacier (Pritchard et al., 2012). Increased discharge of cold water from shrinking ice shelves has also been related to increases in the extent of Antarctic sea ice, which may offset projected future precipitation increases around Antarctica in a warming climate (Winkelmann et al., 2012; Bintanja et al., 2013). Oceanic warming in Antarctica has been linked to increases in the upwelling of warm Circumpolar Deep Water, which melts tidewater glaciers and ice shelves from below (Pritchard et al., 2012). Upwelling of Circumpolar Deep Water, in association with El Niño–Southern Oscillation (ENSO) and Southern Annular Mode climatic oscillations, is projected to continue, raising questions regarding the dynamic response of ice sheets and ice streams to these changes.

Predicting the wider future response of the Antarctic Ice Sheet to climate change therefore requires understanding of the ice streams that dominate its dynamics. Changes in dynamical ice-stream behaviour are a first-order control on rates of deglaciation and meltwater discharge to the oceans, both now and in the immediate future (Gregoire et al., 2012). Although there is abundant marine geological evidence that, at the Last Glacial Maximum (LGM), the Antarctic Peninsula Ice Sheet was drained by ice streams (Davies et al., 2012a), little is known about ice-stream dynamical behaviour, including the timing of ice-stream initiation, ice-stream duration and the rate of ice-stream thinning (Livingstone et al., 2012). Marine geological studies (for example, Ó Cofaigh et al. 2005, 2008; Graham and Smith 2012) also provide only a snapshot of ice-stream behaviour during deglaciation (Bentley and Anderson, 1998; Evans et al., 2005, Heroy and Anderson, 2007; Graham et al. 2009).

Constructing ice sheet chronologies from marine geological evidence is problematic because of the large marine reservoir effect that hinders radiocarbon dating (Davies et al., 2012a). An alternative approach in Antarctica is to use isolated coastal and inland nunataks as “dipsticks” to measure vertical changes in the ice sheet using cosmogenic nuclide methods (Bentley et al., 2006; Mackintosh et al., 2007; Balco et al., 2011, 2013). This dipstick approach has yielded important data about vertical changes in the Antarctic Ice Sheet above its present surface elevation. Questions of ice sheet thickness and ice stream dynamical behaviour therefore rely on glacial geology investigations on nunataks and ice-free ground, but this is difficult as ~99% of the Antarctic continent is glacierised. The Ulu Peninsula, James Ross Island, is one of the largest ice-free areas on the north-east Antarctic Peninsula, and it preserves a detailed record of glacial fluctuations. The aim of this paper is therefore to use cosmogenic isotope exposure-age dating of terrestrial erratic boulders on ice-free land on James Ross Island, north-eastern Antarctic Peninsula, to define the evolution of Last Glacial Maximum (LGM) ice in the Prince Gustav Channel region between Trinity Peninsula and James Ross Island (Fig. 1).

STUDY AREA

During the LGM, at ~18 ka, ice draining from the north-eastern Antarctic Peninsula coalesced with the Mount Haddington Ice Cap on James Ross Island (Bentley and Anderson, 1998; Camerlenghi et al., 2001; Evans et al., 2005; Heroy and Anderson, 2007; Johnson et al. 2011; Davies et al., 2012a). Isotopic evidence from an ice core on Mount Haddington (see Fig. 1 for location) indicates that it existed as an independent ice dome throughout the LGM, and was not overrun by isotopically colder ice from Trinity Peninsula (Mulvaney et al., 2012). Ice coalesced from the Mount Haddington Ice Cap and accumulation areas on Trinity Peninsula to form a palaeo-ice stream flowing northwards and

southwards to the continental shelf edge, with an ice divide in central Prince Gustav Channel. The geological record of Prince Gustav Ice Stream is largely derived from marine sediment cores and swath bathymetry, which reveal subglacial tills and mega-scale glacial lineations in Prince Gustav Channel and Vega Basin (Fig. 1) (Camerlenghi et al., 2001; Evans et al., 2005). The LGM history of the Antarctic Peninsula Ice Sheet and its post-LGM recession is reconstructed here using cosmogenic isotope exposure-age dating of erratic boulders transported by the Antarctic Peninsula Ice Sheet onto James Ross Island (Figs 1 and 2).

Ulu Peninsula on James Ross Island is largely ice-free, with several small glaciers and ice domes on flat-topped volcanic mesas. It is uniquely placed to provide a terrestrial record of the dynamics of the LGM ice sheet because Trinity Peninsula and James Ross Island are geologically distinct (Fig. 1). The Antarctic Peninsula is dominated by Permo-Triassic metamorphic rocks of the Trinity Peninsula Group, into which are intruded granitic rocks (Aitkenhead, 1975; Smellie et al., 1996). James Ross Island is formed entirely of Cretaceous sedimentary rocks and unconsolidated sediments, overlain by the cliff-forming Neogene basaltic James Ross Island Volcanic Group, with glacigenic strata (diamictites) at the base and within (Pirrie et al., 1997; Hambrey and Smellie, 2006; Hambrey et al., 2008; Smellie et al., 2008, 2013). Lavas in the James Ross Island Volcanic Group are flood basalts associated with hyaloclastite deltas that together form flat-topped mesas above the Cretaceous strata (Nelson, 1975; Nývlt et al., 2011; Smellie et al., 2013). Granitic and metamorphic erratic boulders from Trinity Peninsula (Bibby, 1966; Nelson et al., 2009; Riley et al., 2011) record incursions of Trinity Peninsula ice onto James Ross Island (Hambrey and Smellie, 2006; Hambrey et al., 2008; Johnson et al., 2011; Fig. 2).

Climatic records indicate that the region has been warming since the 1930s (Vaughan et al. 2003), although ice-core records suggest that warming began 600 years ago (Mulvaney et al. 2012), with summer snow-melt accelerating during the twentieth century (Abram et al. 2013). This warming has been associated with changes in the westerly winds around Antarctica, which produce warming over the Antarctic Peninsula. Most land-terminating glaciers on Ulu Peninsula are receding (Carrivick et al., 2012; Davies et al., 2012b; Engel et al., 2012), with up to 100 m of recession since their most recent readvance. These glaciers are surrounded by prominent ice-cored moraines (Carrivick et al., 2012; Davies et al., 2013). More widely, tidewater glaciers around the northern Antarctic Peninsula are also shrinking in response to continued atmospheric warming (Davies et al. 2012b), which also resulted in the collapse of Prince Gustav Ice Shelf in 1995 (Skvarca et al. 1995; Cooper, 1997).

METHODS

Cosmogenic nuclide exposure-age dating

Sampling strategy

Cosmogenic isotope dating of glacially transported and erratic boulders is now a widely accepted method for dating glacigenic landforms such as moraines, where it is possible to use crest-line boulders to establish the age of moraine formation (Gosse and Phillips, 2001; Cockburn and Summerfield, 2004; Balco, 2011; Applegate et al., 2012). It is particularly useful in Antarctica, where there are few terrestrial organic remains and the large marine-reservoir effect makes conventional radiocarbon dating difficult (Ingólfsson, 2004; Davies et al., 2012a). The high winds and arid climate reduce the probability of perpetual burial by drifting snow or sediment (Bentley et al., 2006;

Mackintosh et al., 2007). However, Antarctic glaciers are frequently cold-based or polythermal, and may be frozen to their beds. Glacially transported boulders and overridden bedrock surfaces may therefore suffer little erosion, and thus retain an inherited cosmogenic nuclide signal. Additionally, in the study area on James Ross Island, granite erratics may be reworked from much older Neogene diamictites (Nývlt et al., 2011). We therefore collected and analysed granitic samples for both ^{26}Al and ^{10}Be and show our results on plots of ^{26}Al/^{10}Be versus ^{10}Be to discriminate samples that may be reworked from Neogene diamictites (cf. Bentley et al., 2006; Wilson et al., 2008).

Samples were collected following the guidelines of Gosse and Phillips (2001) and Balco (2011). We sampled boulders with a *b*-axis >1.0 m wherever possible (Tables 1 and 2; Figure 3) because using larger boulders reduces the possibility of burial or exhumation during periglacial recycling of clasts within the active layer. Larger boulders standing proud on the land surface are also likely to be wind-scoured and therefore clear of snow during the winter. Only boulders on stable moraine crests were sampled, avoiding boulders on uneven or unstable surfaces, which may have moved since deposition. Samples were collected only from the upper surfaces of the boulders using a hammer and chisel, and all samples were less than 5 cm thick (considerably less for many of the granite boulders, which generally produced >1 cm thick surface flakes when sampled). Detailed site descriptions (e.g. geomorphological context, surrounding sediment texture, boulder dimensions, weathering characteristics) were made for each sample. Sample locations were recorded using a hand-held GPS, accurate to ±5 m in the horizontal dimension. Skyline measurements were collected with a compass-clinometer at all sites to check for possible topographic shielding (i.e. to check if the angle to the horizon was greater than 20^{o}). To avoid complexities associated with possible marine inundation and recent iceberg transportation, all boulders were collected from sites above 30 metres above sea level (m a.s.l.), the highest regional Holocene marine level (Hjort et al., 1997; Fretwell et al., 2010).

Chemical analysis

The granite boulders yielded quartz, which was analysed with ^{10}Be and ^{26}Al, and basalt boulders were crushed and the whole-rock chemistry was analysed for ^{36}Cl. The sample preparation and ^{10}Be/^{26}Al measurement procedures followed standard protocols (Wilson et al., 2008; Glasser et al., 2009; Ballantyne et al., 2009). We added 250 µg Be to each sample as a carrier. Inherent Al concentrations in quartz were determined with an ICP-OES at the Scottish Universities Environmental Research Centre (SUERC). An aluminium carrier was added to most samples so that 2 mg Al per sample was reached.

The ^{10}Be and ^{26}Al exposure ages and internal uncertainties (Tables 1 and 2) were calculated with the CRONUS-earth online calculators version 2.2 (http://hess.ess.washington.edu/math/; Wrapper script: 2.2; Main calculator: 2.1; Objective function: 2; Constants: 2.2.1; Muons: 1.1; see Balco et al. 2008). Because production rates vary globally, Table 3 provides ^{10}Be and ^{26}Al ages calculated using the mid-latitude southern hemisphere New Zealand calibration dataset for reference and completeness (Putnam et al., 2010).

Samples for ^{36}Cl analysis were crushed, sieved to 125–250 µm, enriched in pyroxene by magnetic separation, and leached in hot 2 M HNO3 to remove meteoric ^{36}Cl contamination. Each sample was then split into two fractions: c. 2 g for elemental analysis and c. 20 g for analysis of ^{36}Cl with

accelerator mass spectrometry (AMS). ICP-OES and ICP-MS measurements were used to determine the Ca, K, Ti, Fe, U, Th and REE contents. Chlorine was extracted and purified to produce AgCl for AMS analysis according to the procedures described in Vincent et al. (2010). A high $^{35}Cl/^{37}Cl$ carrier was used to determine the total Cl concentration by AMS Isotope Dilution technique (AMS-ID; Di Nicola et al., 2009).

^{36}Cl exposure ages and internal uncertainties were calculated according to Schimmelpfennig et al. (2009). Sea level-high latitude ^{36}Cl production rates of 48.8±3.4, 162±25,13±3 and 1.9±0.2 atoms ^{36}Cl g^{-1} a^{-1}, from Ca, K, Ti and Fe respectively, were used (Schimmelpfennig et al., 2009) and scaled according to the Stone (2000) scaling scheme. The time-independent Lal/Stone scheme was chosen to be consistent with calculated ^{36}Cl ages and other ages published for the Antarctic Peninsula (Bentley et al., 2006; Davies et al., 2012a).

Calculation of uncertainties

Primary Standards NIST-SRM4325, PRIME-Z92-0222 and PRIME-Z93-0005, with nominal ratios 2.79E-11 $^{10}Be/Be$, 4.11E-11 $^{26}Al/Al$ and 1.2E-12 $^{36}Cl/Cl$, were used for the AMS measurements (Freemnan et al., 2004). These agree with those prepared by Nishiizumi *et al.* (2007), which were used as secondary standards. The reported uncertainties of the cosmonuclide concentrations include 2.5% for the AMS and chemical preparation. Blank corrections ranged between 4 and 11% for $^{10}Be/Be$ ratios; between 0.1 and 3.2% for $^{26}Al/Al$ ratios; and between 5 and 7% for $^{36}Cl/Cl$ ratios. These corrections are included in the stated uncertainties.

RESULTS: GLACIAL GEOLOGY AND GEOMORPHOLOGY

Ulu Peninsula is characterised by several small cirque and valley glaciers, with ice domes on flat-topped volcanic mesas (Figs. 2, 3A, 3B). On the tops of the mesas (above 370 m a.s.l.), the flood basalts and hyaloclastite deltas have been broken down to form blockfields where periglacial action is evident. Rare isolated granite boulders occur in these locations (Fig 3B). The interior of Ulu Peninsula is widely mantled by an erratic-poor, basaltic pebble-cobble gravel. Subangular pebbles and cobbles form a lag on the surface, with frequent basalt and rare granitic boulders. This surface has been deflated, and fine to coarse sand is present beneath the pebble lag (Fig. 3E). There is evidence of localised stone-sorting by periglacial processes in these areas (Davies et al., 2013).

Coastal areas, both to the west and east of Ulu Peninsula, are commonly characterised by glacigenic deposits with far higher proportions of Trinity Peninsula erratic material, and with many more large granite boulders. Some of this drift is associated with moraine fragments (for example at Kaa Bluff and St Martha Cove; Figs. 2, 3C, 3D). Large (up to 2 m *b*-axis) Trinity Peninsula granite boulders and sub-rounded, striated, faceted, glacially transported, locally derived boulders are scattered widely across the surface of Ulu Peninsula (Fig. 2). Together with streamlined bedrock ridges, smoothed and sculpted cols and passes, the glacial drifts indicate that the area was inundated by the Antarctic Peninsula Ice Sheet.

RESULTS: COSMOGENIC ISOTOPE DATING

Cosmogenic ^{26}Al and ^{10}Be data from granite erratic boulders and ^{36}Cl from locally derived glacially transported basalt boulders on James Ross Island indicate the timing and duration of deglacial ice-streaming events (Figs. 2, 4; Tables 1 and 2). The $^{26}Al/^{10}Be$ ratios of all granite samples were

statistically equal to or greater than the production rate ratio (Fig. 5), suggesting that they have been constantly exposed and not subjected to repeated burial and exhumation, which may be an issue in cold Antarctic environments (Bentley et al., 2006) and where there is the potential for reworking of older Neogene glacial deposits (Nývlt et al., 2011). Boulder ages are presented as a weighted mean of the ^{26}Al and ^{10}Be ages (Wilson et al., 2008). Following the convention in Antarctica, we use the oldest age in cases where there is geological scatter in the sample ages because boulders may slip downslope, rotate, or be shielded by snow (Balco et al., 2011). This method is appropriate because the co-isotope plot suggests that inheritance is not a problem in the samples.

Two large white granite boulders embedded on the summit of Lachman mesa at 370 metres above sea level (JRI49 and JRI50; Figs. 2, 4; Table 1) yielded cosmogenic isotope ages of 17.7 ± 0.8 and 15.1 ± 0.4. Near Davies Dome, basalt samples JRI33 and JRI34 yield ^{36}Cl ages of 19.9 ± 7.2 and 22.1 ± 6.6 ka (Fig. 2). These ages indicate that the age of deglaciation of Lachman mesa is ~ 18 ka, synchronous with the observed ice-sheet recession across the continental shelf (Heroy and Anderson, 2005; 2007). Somewhat younger deglaciation ages of 11.8 and 13.8 ka were obtained for basalt bedrock at Crisscross Crags and Patalamon Mesa (Figure 1), at c. 600 m elevation, by Johnson et al. (2009). However, the younger ages probably relate to the persistence of local ice domes (both localities sustain ice domes today) that took longer to decay and expose bedrock than at Lachman mesa.

In the most northerly part of Ulu Peninsula, a lower elevation sample (JRI35) in the granite-rich drift (45 m.a.s.l.) on Cape Lachman on the NW of James Ross Island, provides an exposure age of 6.3 ± 0.2 ka. South of Brandy Bay, samples JRI01 and JRI03, which are large granite erratic boulders in the coastal erratic-rich drift at elevations of ~100 m.a.s.l. on "San Carlos Hill", south of San Carlos Point (Fig. 2), provide exposure ages of 12.2 ± 0.4 and 11.3 ± 0.4 ka respectively. A large granite erratic boulder in Sharp Valley, NW of James Ross Island (JRI09), provides a cosmogenic isotope age of 8.9 ± 0.2 ka. Further west, sample JRI 62 collected at Kaa Bluff at 144 m.a.s.l. (Figs. 3C, 4), NW James Ross Island, indicates that Peninsula ice receded from James Ross Island around 7.6 ± 0.3 ka. In the interior of Ulu Peninsula, sample JRI26 is an isolated granite boulder, located on a basalt drift at San Jose Pass, which indicates ice recession at 6.7 ± 0.3 ka. On the eastern side of the island, a granite erratic boulder in granite-rich drift on a subdued, degraded moraine ridge (sample JRI29 at St. Martha Cove, Fig. 2) was dated to 6.1 ± 0.3 ka.

DISCUSSION: IMPLICATIONS FOR THE LAST GLACIAL MAXIMUM ANTARCTIC ICE SHEET

The location of the erratic boulders and their exposure ages indicate that at ~18 ka, a relatively thick Antarctic Peninsula Ice Sheet deposited erratic boulders derived from Trinity Peninsula at elevations of up to ~370 m a.s.l. on James Ross Island (our data) and on Seymour Island (Johnson et al., 2011). Subsequent surface-lowering of the LGM ice sheet is indicated by the younger exposure ages at lower elevations. This surface-lowering marks a dynamical change coincident with the onset of the LGM Prince Gustav Ice Stream. This dynamical change occurred after ~18 ka but before 12.2 ± 0.4 ka, which is the exposure age of the oldest erratic boulder (JRI01) in the coastal erratic-rich drift of the Ulu Peninsula (Fig. 2). The coastal erratic-rich drift is interpreted as demarking a region of enhanced wet-based glacial deposition (Davies et al., 2013), which, combined with the offshore lineations mapped in Vega Basin (Evans et al., 2005; Camerlenghi et al., 2001; Fig. 2) is interpreted as the lateral margin of the Prince Gustav Ice Stream. Sample JRI62 is located on a moraine fragment on Kaa Bluff at 144 m.a.s.l., and this location effectively delimits the maximum height of the lateral margins of the

Prince Gustav Ice Stream. The ice surface therefore lowered at least 230 m during the interval 18 to 12.2 ka. Younger ages for granite erratic boulders occupying low-lying coastal sites on western Ulu Peninsula indicate that the ice stream continued to impinge on the shores of James Ross Island until ~7 ka. Local ice from Mount Haddington Ice Cap remained on Ulu Peninsula, flowing east out of St. Martha Cove until 6.1 ± 0.3 ka. An ice-sheet configuration similar to that of today was achieved after ~6 ka.

These data are supported by field observations and cosmogenic-nuclide exposure ages from ice-free areas adjacent to the Sjögren, Boydell, and Drygalski Glaciers on the north-eastern Antarctic Peninsula (Fig. 1), where the LGM ice-surface elevation near the present coastline was ~500 m a.s.l., with cold-based ice at elevations above 100-150 m a.s.l., and wet-based ice below (Balco et al., 2013). The ice-surface elevation decreased from ~500 m a.s.l. to near present-day sea-level between 9 ka and ~4 ka, confirming previous interpretations that deglaciation took place between >14 ka and ~6 ka (Ingólfsson et al., 2003). The minimum age for deglaciation in Prince Gustav Channel is 10.6 cal. ka BP, following a period of rapid warming recorded in the James Ross Island ice core (Figs. 1 and 6; Mulvaney et al., 2012). These data confirm our estimate of 144 m a.s.l. for the Prince Gustav Ice Stream at 7.6 ± 0.3 ka and complete withdrawal of the ice stream from Ulu Peninsula by ~6 ka. Radiocarbon ages from glaciomarine sediments in southern Prince Gustav Channel (Fig. 1) indicate ice-free conditions here by ~9 cal. ka BP (Pudsey and Evans, 2001). Published exposure ages Johnson Mesa (260-304 m a.s.l.) and Terrapin Hill (80-85 m a.s.l.) from James Ross Island (Fig. 1) also indicate the recession of Prince Gustav Ice Stream and imply deglaciation in Prince Gustav Channel around 6-8 ka (Johnson et al., 2011).

Deglaciation in early Holocene time is also indicated by the relative sea-level record at Beak Island, north of Ulu Peninsula (Figs. 1, 6), which became ice-free with the onset of glaciomarine sedimentation at 10.7 cal. ka BP (Roberts et al., 2011). A sea level high-stand at 8 cal. ka BP indicates rapid eustatic sea-level rise, which outpaced isostatic readjustment at this time. The Beak Island sea-level record agrees with other published sea-level data in this region (Hjort et al., 1997) and with isostatically coupled sea-level models (Huybrechts, 2002; Peltier, 1998). These relative sea-level data confirm the interpretation of rapid ice-stream thinning, recession and drawdown during a period of rapid warming in the early Holocene Epoch (cf. Mulvaney et al., 2012; Fig. 6).

On the western Antarctic Peninsula, oxygen isotope data from diatoms in marine sediment cores in the Palmer Deep indicate that the period from 13.0-12.1 ka was characterised by rapid deglaciation, coincident with ice-stream retreat in the outer and inner Anvers Trough, the breakup of Marguerite Bay ice shelf and decreases in sea ice in Maxwell Bay (Pike et al., 2013). Our study shows that by 12 ka, the Prince Gustav Ice Stream on the eastern Antarctic Peninsula was already thinning and receding, suggesting that ice-stream response was coincident on both the western and eastern Antarctic Peninsula. This region-wide glacier recession has been linked to increased upwelling of upper Circumpolar Deep Water onto the continental shelf, associated with strong winds in the Southern Ocean westerlies (Pike et al., 2013). After 12 ka, a slow-down in glacial recession is noted by decreased glacial discharge both in the Palmer Deep (Pike et al., 2013), and in the slower recession of Prince Gustav Ice Stream around Ulu Peninsula. The final recession of Prince Gustav Ice Stream around 7.6 ka is also coincident with increased upwelling of Circumpolar Deep Water.

These changes in the upwelling of Circumpolar Deep Water have been related to variations in ENSO as well as the Southern Annular Mode (Pike et al., 2013), and recent increases in summer melt on James Ross Island have also been related to a strengthening of the Southern Annular Mode (Abram et al., 2013). Our new data on previous ice-stream response to past climatic variations confirm that the north-eastern Antarctic Peninsula is a dynamic environment, sensitive to small changes in oceanic and atmospheric circulation. This has important implications for future ice dynamics as global atmospheric temperatures approach those of the mid-Holocene climatic optimum (Marcott et al., 2013).

CONCLUSIONS

Cosmogenic isotope dating of granite and basalt erratic boulders indicates a three-phase LGM ice-sheet evolution on James Ross Island (Fig. 6). Firstly, until ~18 ka James Ross Island was inundated by a thick Antarctic Peninsula Ice Sheet. An important change occurred after ~18 ka when the ice sheet became more dynamic. The development of the Prince Gustav Ice Stream resulted in lowering of the regional ice-sheet surface. Secondly, ice-sheet thinning and the onset of Prince Gustav Ice Stream from 18-12 ka coincided with rapid eustatic sea-level rise (Roberts et al., 2011) and rapidly increasing air temperatures recorded in the Mount Haddington ice cores (Fig. 1; Mulvaney et al., 2012). Finally, after ~8 ka, rapid isostatic uplift produced falling relative sea level, coincident with ice-stream recession and deglaciation of Ulu Peninsula. By 6 ka, ice sheet configuration was similar to present. We conclude that ice streams exerted a strong control on the deglaciation of the LGM Antarctic Peninsula Ice Sheet. Although deglacial ice-stream initiation has been inferred for former mid-latitude ice sheets, this is the first robustly dated example of Antarctic ice-stream initiation, duration and thinning.

ACKNOWLEDGEMENTS

This work was funded by the UK Natural Environment Research Council (NERC) under the Antarctic Funding Initiative NE/F012942/1). Transport, logistics and fieldwork on James Ross Island were supported by the British Antarctic Survey, and we thank the captain and crew of the *RRS Ernest Shackleton* and the *RRS James Clark Ross* for their support. We thank Alan Hill for his field logistical support. ^{10}Be, ^{26}Al and ^{36}Cl analyses were supported by a NERC CIAF grant (9035/0407), and we also acknowledge Joyce Wilcox and Allan Davidson (both SUERC) for help with these analyses.

FIGURE CAPTIONS

Figure 1. Geographical and geological context of James Ross Island and Trinity Peninsula, with bathymetric data (50 m resolution). Inset shows wider location of James Ross Island. Previously published ages are from Hjort et al. (1997), Pudsey and Evans (2001), Heroy and Anderson (2005; 2007), Johnson et al. (2009, 2011) and Balco et al. (2013). Circles are calibrated radiocarbon ages (ka BP) and diamonds are ^{10}Be cosmogenic nuclide exposure ages (ka). Mega-scale glacial lineations are shown in Prince Gustav Channel. JRIVG = James Ross Island Volcanic Group. Location of Fig. 2 is indicated.

Figure 2. Geomorphological map of Ulu Peninsula showing sample location and ID with cosmogenic nuclide ages in bold (green stars and triangles). Ages are in ka. The coastal 'erratic-rich drift', which denotes the lateral margins of Prince Gustav Ice Stream, is indicated by cross-hatching. Red circles indicate mapped granite erratic boulders with a b-axis > 1 m. Large, prominent ice-cored moraines occur around modern cirque glaciers, and a large moraine flanks Brandy Bay. Degraded ridges, interpreted as moraine fragments, occur at Kaa Bluff and St. Martha Cove. Previously published cosmogenic nuclide exposure ages are shown. Spot heights are given in metres above sea level (in italics).

Figure 3. A) Ulu Peninsula from Johnson Mesa. Note the flat-topped volcanic mesas with small ice domes, small cirque glaciers and smooth terrain. B) Cosmogenic nuclide samples JRI 49 on Lachman mesa. An isolated granite boulder on a volcanic blockfield. C) Moraine below Kaa Bluff, with a distinct ridge with numerous white granite boulders and cobbles. Sample JRI 62 in the foreground. D) Cape Lachman, northern promontory on James Ross Island. Numerous granite boulders are present in the saddle at the neck of the promontory. E) Looking down towards the Abernethy Flats, with a boulder-train of Holocene age in the foreground and rare granite boulders.

Figure 4. James Ross Island boulder samples, showing context and age (ka). The first four boulders are situated at high elevations on mesa surfaces. Samples JRI26 and JRI29 are situated in San Jose Pass and St. Martha Cove respectively, and document the recession of ice across the interior of the Ulu Peninsula. The remaining samples are from erratic-rich drifts deposited by the Prince Gustav Ice Stream, which receded in a south-westerly direction from Cape Lachman (12 - 13 ka) to San Carlos Hill (~12 ka) and back towards Kaa Bluff (~7 ka).

Figure 5. Co-isotope plot of ^{26}Al/^{10}Be versus ^{10}Be. Theoretical cosmogenic concentrations in a surface affected by no erosion and in a surface in erosion equilibrium are depicted by black lines according to CRONUS production rates. External uncertainties of these lines as a result of a 6% error in both ^{10}Be and ^{26}Al production rates are represented by the grey areas. No samples plot in the zone of complex exposure, indicating that the samples have not been buried for a substantial period of time and then exhumed.

Figure 6. A) Local temperature changes from the Mount Haddington ice core (see Fig. 1 for location) (Mulvaney et al., 2012). Temperature anomaly compared with 1961-1990 mean; 100-year average. B) Relative sea level (RSL) curve for Beak Island, Prince Gustav Channel (Fig. 1; Roberts et al., 2011) and a suite of coupled sea-level models (Peltier, 1998; Huybrechts, 2002), and marine microfossils from James Ross Island (Ingólfsson et al., 1992; Hjort et al., 1997). C) Sample altitude and mean age

393 showing ice-sheet thinning, and the cluster of ^{10}Be ages related to the recession of Prince Gustav Ice
394 Stream (this study). Triangles indicate granite boulders on basalt-rich lag surfaces at high elevations
395 (>360 m a.s.l.) (4 samples) deposited by a thick, cold Antarctic Peninsula Ice Sheet. Diamonds
396 indicate Trinity Peninsula erratic boulders on coastal areas of James Ross Island within the erratic-rich
397 drift (5 samples), deposited by Prince Gustav Ice Stream. Squares (2 samples) indicate lower
398 elevation samples deposited by the thinning ice sheet in the interior of Ulu Peninsula. The period of
399 rapid ice-sheet thinning and onset of Prince Gustav Ice Stream observed on Ulu Peninsula coincides
400 with rapid regional temperature increases and rapid eustatic sea-level rise; the youngest deglaciation
401 ages coincide with a period of rapid isostatic uplift on nearby Beak Island (Fig. 1; Roberts et al.,
402 2011).
403
404

TABLE CAPTIONS

Table 1. Sample details used to calculate ^{10}Be ages in the Cronus-earth online calculators (Balco et al. 2008).

Table 2. Summary of new cosmogenic nuclide ages from Ulu Peninsula. The ^{10}Be ages are presented in the text and figures because the ^{26}Al/^{10}Be ratios are statistically equal or greater than the production ratio, suggesting no complex exposure or burial history. JRI = James Ross Island, APIS = Antarctic Peninsula Ice Sheet.

Table 3. Calculations of ^{10}Be ages using the Cronus-earth online calculator (Balco et al. 2008) with the New Zealand-Macaulay calibration dataset (Putnam et al., 2010) and the global time-independent Lal/Stone scheme. There is a difference of ~16% between the ages when calculated using these different production rates.

REFERENCES

Abram, N.J., Mulvaney, R., Wolff, E.W., Triest, J., Kipfstuhl, S., Trusel, L.D., Vimeuz, F., Fleet, L. and Arrowsmith, C. 2013. Acceleration of snowmelt in an Antarctic Peninsula ice core during the twentieth century. *Nature Geoscience* doi:10.1038/ngeo1787.

Aitkenhead, N., 1975. The geology of the Duse Bay—Larsen Inlet area, north-east Graham Land (with particular reference to the Trinity Peninsula Series). *British Antarctic Survey Scientific Reports* 51, 1-62.

Applegate, P. J., Urban, N. M, Keller, K., Lowell, T. V., Laabs, B. J. C., Kelly, M. A., and Alley, R. B., 2012. Improved moraine age interpretations through explicit matching of geomorphic process models to cosmogenic nuclide measurements from single landforms. *Quaternary Research* 77, 293-304.

Balco, G.A. 2011. Contributions and unrealized potential contributions of cosmogenic-nuclide exposure dating to glacier chronology, 1990-2010. *Quaternary Science Reviews* 30, 3-27.

Balco, G.A., Schaefer, J.M. and LARISSA Group. 2013. Exposure-age record of Holocene ice sheet and ice-shelf change in the northeast Antarctic Peninsula. *Quaternary Science Reviews* 59, 101-111.

Ballantyne, C.K., Schnabel, C. and Xu, S. 2009. Exposure dating and reinterpretation of coarse debris accumulations ('rock glaciers') in the Cairngorm Mountains, Scotland. *Journal of Quaternary Science* 24, 19-31.

Barrand, N. E., Vaughan, D. G., Steiner, N., Tedesco, M., Kuipers Munneke, P., van den Broeke, M. R., and Hosking, J. S. (2013). Trends in Antarctic Peninsula surface melting conditions from observations and regional climate modeling. *Journal of Geophysical Research: Earth Surface* **118** (1), 315-330.

Bentley, M.J. and Anderson, J.B., 1998. Glacial and marine geological evidence for the ice sheet configuration in the Weddell Sea-Antarctic Peninsula region during the Last Glacial Maximum. *Antarctic Science* 10, 309-325.

Bentley, M.J., Fogwill, C.J., Kubik, P.W. and Sugden, D.E. 2006, Geomorphological evidence and cosmogenic $^{10}Be/^{26}AL$ exposure ages for the Last Glacial Maximum and deglaciation of the Antarctic Peninsula Ice Sheet. *Geological Society of America Bulletin* 118, 1149-1159.

Bibby, J.S., 1966, *The stratigraphy of part of north-east Graham Land and the James Ross Island Group*, 37 British Antarctic Survey, London.

Bintanja, R., van Oldenborgh, G.J., Drijfhout, S.S., Wouters, B. and Katsman, C.A. 2013, Important role for ocean warming and increased ice-shelf melt in Antarctic sea-ice expansion. *Nature Geoscience* 6, 376-379**.**

Camerlenghi, A., Domack, E., Rebesco, M., Gilbert, R., Ishman, S., Leventer, A., Brachfeld, S. and Drake, A., 2001. Glacial morphology and post-glacial contourites in northern Prince Gustav Channel (NW Weddell Sea, Antarctica). *Marine Geophysical Researches* 22, 417-443.

Carrivick, J.L., Davies, B.J., Glasser, N.F. and Nývlt, D. 2012. Late Holocene changes in character and behaviour of land-terminating glaciers on James Ross Island, Antarctica. *Journal of Glaciology* 58, 1476-1490.

Cockburn, H.A.P. and Summerfield, M.A. 2004. Geomorphological applications of cosmogenic isotope analysis. *Progress in Physical Geography* 28, 1-42.

Cook, A.J., Fox, A.J., Vaughan, D.G. and Ferrigno, J.G., 2005. Retreating glacier fronts on the Antarctic Peninsula over the past half-century. *Science* 308 (5721), 541-544.

Cook, A.J. and Vaughan, D.G., 2010. Overview of areal changes of the ice shelves on the Antarctic Peninsula over the past 50 years. *The Cryosphere* 4, 77-98.

Cooper, A.P.R., 1997. Historical observations of Prince Gustav Ice Shelf. *Polar Record* 33, 285-294.

Davies, B.J., Hambrey, M.J., Smellie, J.L., Carrivick, J.L. and Glasser, N.F. 2012a. Antarctic Peninsula Ice Sheet evolution during the Cenozoic Era. *Quaternary Science Reviews* 31, 30-66.

Davies, B.J., Carrivick, J.L., Glasser, N.F., Hambrey, M.J. and Smellie, J.L. 2012b. Variable glacier response to atmospheric warming, northern Antarctic Peninsula, 198802009. *The Cryosphere* 6, 1031-1048.

Davies, B.J., Glasser, N.F., Carrivick, J.L., Hambrey, M.J., Smellie, J.L. and Nývlt, D. 2013. Landscape evolution and ice-sheet behaviour in a semi-arid polar environment: James Ross Island, NE Antarctic Peninsula. in *Antarctic Palaeoenvironments and Earth Surface Processes*, Vol. 381 (eds. Hambrey, M.J., Barker, P.F., Barrett, P.J., Bowman, V.C., Davies, B.J., Smellie, J.L. and Tranter, M.) Geological Society of London, Special Publications, London.

Di Nicola, L, Schnabel, C, Wilcken, KM, and Gméling, K 2009. Determination of chlorine concentrations in whole rock samples with prompt-gamma activation analysis (PGAA) and isotope dilution AMS. *Quaternary Geochronology* 4, 501-507.

Engel, Z., Nývlt, D., and Láska, K., 2012. Ice thickness, areal and volumetric changes of Davies Dome and Whisky Glacier (James Ross Island, Antarctic Peninsula) in 1979-2006. *Journal of Glaciology* 58, 904-914.

Evans, J., Pudsey, C.J., Ó Cofaigh, C., Morris, P. and Domack, E. 2005. Late Quaternary glacial history, flow dynamics and sedimentation along the eastern margin of the Antarctic Peninsula Ice Sheet. *Quaternary Science Reviews* 24, 741-774.

Freeman, S., Xu, S., Schnabel, C., Dougans, A., Tait, A., Kitchen, R., Klody, G., Loger, R., Pollock, T., Schroeder, J., Sundquist, M. 2004. Initial measurements with the SUERC accelerator mass spectrometer. *Nuclear Instruments and Methods in Physics Research Section B: Beam Interactions with Materials and Atoms*, 223–224, 195 – 198.

Fretwell, P.T., Hodgson, D.A., Watcham, E.P., Bentley, M.J. and Roberts, S.J. 2010. Holocene isostatic uplift of the South Shetland Islands, Antarctic Peninsula, modelled from raised beaches. *Quaternary Science Reviews* 29, 1880-1893.

Glasser, N.F., Clemmens, S., Schnabel, C., Fenton, C.R. and Mchargue, L. 2009. Tropical glacier fluctuations in the Cordillera Blanca, Peru between 12.5 and 7.6 ka from cosmogenic Be-10 dating. Q*uaternary Science Reviews* 28, 3448-3458.

Gosse, J.C. and Phillips, F.M. 2001. Terrestrial in situ cosmogenic nuclides: theory and application. *Quaternary Science Reviews* 20, 1475-1560.

Graham, A.G.C., Larter, R.D., Gohl, K., Hillenbrand, C.-D., Smith, J.A. and Kuhn, G. 2009. Bedform signature of a West Antarctic palaeo-ice stream reveals a multi-temporal record of flow and substrate control. *Quaternary Science Reviews* 28, 2774-2793.

Graham, A.G.C. and Smith, J.A. 2012. Palaeoglaciology of the Alexander Island ice cap, western Antarctic Peninsula, reconstructed from marine geophysical and core data. *Quaternary Science Reviews* 35, 63-81.

Gregoire, L.J., Payne, A.J. and Valdes, P.J. 2012. Deglacial rapid sea level rises caused by ice sheet saddle collapses. *Nature* 487, 219-222.

Hambrey, M.J. and Smellie, J.L. 2006. Distribution, lithofacies and environmental context of Neogene glacial sequences on James Ross and Vega Islands, Antarctic Peninsula, *in* Francis, E.A., Pirrie, D. and Crame, J.A., eds, Cretaceous-Tertiary High-Latitude Palaeoenvironments, James Ross Basin, Antarctica, 258, 187-200, Geological Society Special Publication, London).

510 Hambrey, M.J., Smellie, J.L., Nelson, A.E. and Johnson, J.S. 2008. Late Cenozoic glacier-volcano
511 interaction on James Ross Island and adjacent areas, Antarctic Peninsula region. *Geological*
512 *Society of America Bulletin* 120, 709-731.
513 Heroy, D.C. and Anderson, J.B. 2005. Ice-sheet extent of the Antarctic Peninsula region during the
514 Last Glacial Maximum (LGM) - Insights from glacial geomorphology: *Geological Society of America*
515 *Bulletin* 117, 1497-1512.
516 Heroy, D.C. and Anderson, J.B. 2007. Radiocarbon constraints on Antarctic Peninsula Ice Sheet retreat
517 following the Last Glacial Maximum (LGM): *Quaternary Science Reviews* 26, 3286-3297.
518 Hjort, C., Ingólfsson, Ó., Möller, P. and Lirio, J.M., 1997. Holocene glacial history and sea-level
519 changes on James Ross Island, Antarctic Peninsula: *Journal of Quaternary Science* 12, 259-273.
520 Huybrechts, P. 2002. Sea-level changes at the LGM from ice-dynamic reconstructions of the
521 Greenland and Antarctic ice sheets during the glacial cycles. *Quaternary Science Reviews* 21,
522 203-231.
523 Ingólfsson, Ó., 2004. Quaternary glacial and climate history of Antarctica. In: J. Ehlers and P.L.
524 Gibbard (Editors), *Quaternary Glaciations - Extent and Chronology, Part III.* Developments in
525 Quaternary Science. Elsevier, pp. 3-43.
526 Ingólfsson, Ó., Hjort, C., Björck, S. and Smith, L.R.I. 1992. Late Pleistocene and Holocene glacial
527 history of James Ross Island, Antarctic Peninsula. *Boreas* 21, 209-222.
528 Ingólfsson, Ó., Hjort, C. and Humlum, O. 2003. Glacial and climate history of the Antarctic Peninsula
529 since the Last Glacial Maximum: *Arctic, Antarctic and Alpine Research* 35, 175-186.
530 Johnson, J.S., Smellie, J.L., Nelson, A.E. and Stuart, F.M. 2009. History of the Antarctic Peninsula Ice
531 Sheet since the early Pliocene—Evidence from cosmogenic dating of Pliocene lavas on James Ross
532 Island, Antarctica. *Global and Planetary Change*, 69, 205-213.
533 Johnson, J.S., Bentley, M.J., Roberts, S.J., Binney, S.A. and Freeman, S.P.H.T. 2011. Holocene deglacial
534 history of the north east Antarctic Peninsula - a review and new chronological constraints:
535 *Quaternary Science Reviews* 30, 3791-3802.
536 Joughin, I., Tulaczyk, S., Bindschadler, R. and Price, S.F. 2002. Changes in west Antarctic ice stream
537 velocities: Observation and analysis. *J. Geophys. Res*. 107 (B11), 2289.
538 Livingstone, S.J., O Cofaigh, C., Stokes, C.R., Hillenbrand, C.-D., Vieli, A. and Jamieson, S.S.R. 2012.
539 Antarctic palaeo-ice streams: *Earth-Science Reviews* 111, 90-128.
540 Mackintosh, A., White, D., Fink, D., Gore, D.B., Pickard, J. and Fanning, P.C. 2007. Exposure ages from
541 mountain dipsticks in Mac. Robertson Land, East Antarctica, indicate little change in ice-sheet
542 thickness since the Last Glacial Maximum. *Geology* 35, 551-554.
543 Marcott, S.A., Shakun, J.D., Clark, P.U. and Mix, A.C. 2013. A Reconstruction of Regional and Global
544 Temperature for the Past 11,300 Years. *Science* 339, 1198-1201.
545 Mulvaney, R., Abram, N.J., Hindmarsh, R.C.A., Arrowsmith, C., Fleet, L., Triest, J., Sime, L.C., Alemany,
546 O. and Foord, S. 2012. Recent Antarctic Peninsula warming relative to Holocene climate and ice-
547 shelf history. *Nature* 489, 141-144.
548 Nelson, P.H.H. 1975. The James Ross Island Volcanic Group of north-east Graham Land. *British*
549 *Antarctic Survey Scientific Reports* 54, 1-62.
550 Nelson, A.E., Smellie, J.L., Hambrey, M.J., Willaims, M. Vautravers, M., Salzmann, U., McArthur, J.M.
551 and Regelous, M. 2009. Neogene glacigenic debris flows on James Ross Island, northern Antarctic
552 Peninsula, and their implications for regional climate history. *Quaternary Science Reviews* 28,
553 3138-3160.

554 Nishiizumi, K., Imamura, M., Caffee, M. W., Southon, J. R., Finkel, R. C., McAninch, J. 2007. Absolute
555 calibration of 10Be AMS standards. *Nuclear Instruments and Methods in Physics Research Section*
556 *B: Beam Interactions with Materials and Atoms,* 258, 403 - 413
557 Nývlt, D., Kosler, J., Mlcoch, B., Mixa, P., Bubik, M. and Hendriks, B.W.H. 2011. The Mendel
558 Formation: Evidence for Late Miocene climatic cyclicity at the northern tip of the Antarctic
559 Peninsula. *Palaeogeography Palaeoclimatology Palaeoecology* 299, 363-384.
560 Ó Cofaigh, C., Dowdeswell, J.A., Allen, C.S., Hiemstra, J.F., Pudsey, C.J., Evans, J. and Evans, D.J.A.,
561 2005. Flow dynamics and till genesis associated with a marine-based Antarctic palaeo-ice stream.
562 *Quaternary Science Reviews* 24, 709-740.
563 Ó Cofaigh, C., Dowdeswell, J.A., Evans, J. and Larter, R.D., 2008. Geological constraints on Antarctic
564 palaeo-ice-stream retreat. *Earth Surface Processes and Landforms* 33, 513-525.
565 Peltier, W.R., 1998. Postglacial variations in the level of the sea: Implications for climate dynamics
566 and solid-Earth geophysics. R*eviews of Geophysics* 36, 603-689.
567 Pike, J., Swann, G.E.A., Leng, M.J. and Snelling, A.M. 2013. Glacial discharge along the west Antarctic
568 Peninsula during the Holocene. *Nature Geoscience* 6, 199-202.
569 Pirrie, D., Crame, J. A., Riding, J. B., Butcher, A. R., and Taylor, P. D. 1997. Miocene glaciomarine
570 sedimentation in the northern Antarctic Peninsula region: the stratigraphy and sedimentology of
571 the Hobbs Glacier Formation, James Ross Island. *Geological Magazine* 134, 745-762.
572 Pritchard, H.D., Ligtenberg, S.R.M., Fricker, H.A., Vaughan, D.G., van den Broeke, M.R. and Padman, L.
573 2012. Antarctic ice-sheet loss driven by basal melting of ice shelves. *Nature* 484, 502-505.
574 Pudsey, C.J. and Evans, J., 2001. First survey of Antarctic sub-ice shelf sediments reveals Mid-
575 Holocene ice shelf retreat. *Geology* 29, 787-790.
576 Putnam, A. E., Schaefer, J. M., Barrell, D. J. A., Vandergoes, M., Denton, G. H., Kaplan, M. R., Finkel, R.
577 C., Schwartz, R., Goehring, B. M. and Kelley, S. E. 2010. In situ cosmogenic 10Be production-rate
578 calibration from the Southern Alps, New Zealand. *Quaternary Geochronology* 5, 392-409.
579 Riley, T.R., Flowerdew, M.J. and Haselwimmer, C.E., 2011. Geological map of Eastern Graham Land,
580 Antarctic Peninsula (1:625 000 scale), BAS GEOMAP 2 Series, Sheet 1 (British Antarctic Survey,
581 Cambridge, UK).
582 Roberts, S.J., Hodgson, D.A., Sterken, M., Whitehouse, P.L., Verleyen, E., Vyverman, W., Sabbe, K.,
583 Balbo, A., Bentley, M.J. and Moreton, S.G., 2011. Geological constraints on glacio-isostatic
584 adjustment models of relative sea-level change during deglaciation of Prince Gustav Channel,
585 Antarctic Peninsula. *Quaternary Science Reviews* 30, 3603-3617.
586 Royles, J., Amesbury, Matthew J., Convey, P., Griffiths, H., Hodgson, Dominic A., Leng, Melanie J.,
587 and Charman, Dan J. (2013). Plants and Soil Microbes Respond to Recent Warming on the
588 Antarctic Peninsula. *Current Biology* **23** (17), 1702-1706.
589 Schimmelpfennig, I., Benedetti, L., Finkel, R., Pik, R., Blard, P.H., Bourles, D., Burnard, P. and Williams,
590 A. 2009. Sources of *in-situ* ^{36}Cl in basaltic rocks. Implications for calibration of production rates.
591 *Quaternary Geochronology* 4, 441-461.
592 Skvarca, P., Rott, H. and Nagler, T. 1995. Satellite imagery, a base line for glacier variation study on
593 James Ross Island, Antarctica. *Annals of Glaciology* 21, 291-296.
594 Smellie, J.L., Roberts, B., and Hirons, S.R. 1996. Very low- and low-grade metamorphism in the Trinity
595 Peninsula Group (Petmo-Triassic) of northern Graham Land, Antarctic Peninsula. *Geological*
596 *Magazine* 133, 583-594.

Smellie, J.L., Johnson, J.S., McIntosh, W.C., Esser, R., Gudmundsson, M.T., Hambrey, M.J. and Van Wyk De Vries, B. 2008. Six million years of glacial history recorded in the James Ross Island Volcanic Group, Antarctic Peninsula. *Palaeogeography, Palaeoclimatology, Palaeoecology* 260, 122-148.

Smellie, J.L., Johnson, J.S. and Nelson, A.E. 2013. Geological map of James Ross Island. 1. James Ross Island Volcanic Group (1:125 000 scale). BAS GEOMAP 2 Series, Sheet 5, British Antarctic Survey, Cambridge, UK.

Stone, J.O. 2000. Air pressure and cosmogenic isotope production. *Journal of Geophysical Research* 105, 23753–23759.

Turner, J., Colwell, S.R., Marshall, G.J., Lachlan-Cope, T.A., Carelton, A.M., Jones, P.D., Lagun, V., Reid, P.A. and Lagovkina, S. 2005. Antarctic climate change during the last 50 years. *International Journal of Climatology* 25, 279-294.

Turner, J., Bindschadler, R., Convey, P., di Prisco, G., Fahrbach, E., Gutt, J., Hodgson, D. A., Mayewski, P. A., and Summerhayes, C. P. (2009). *Antarctic Climate Change and the Environment*. Scientific Committee on Antarctic Research, Cambridge. 555 pp.Vaughan, D.G., Marshall, G.J., Connelly, W.M., Parkinson, C., Mulvaney, R., Hodgson, D.A., King, J.C., Pudsey, C.J. and Turner, J. 2003. Recent rapid regional climate warming on the Antarctic Peninsula. *Climatic Change* 60, 243-274.

Vincent, P. J., Wilson, P.,Lord, T.C., Schnabel, C., Wilcken, K.M. 2010. Cosmogenic isotope (36Cl) surface exposure dating of the Norber erratics, Yorkshire Dales: Further constraints on the timing of the LGM deglaciation in Britain. *Proceedings of the Geologists' Association* 121, 24-31.

Wilson, P., Bentley, M.J., Schnabel, C., Clark, R. and Xu, S. 2008. Stone run (block stream) formation in the Falkland Islands over several cold stages, deduced from cosmogenic isotope (^{10}Be and ^{26}Al) surface exposure dating. *Journal of Quaternary Science* 23, 461-473.

Winkelmann, R., Levermann, A., Martin, M.A. and Frieler, K. 2012. Increased future ice discharge from Antarctica owing to higher snowfall. *Nature* 492, 239-243.

Sample	Date Sampled	Skyline	Lithology	Altitude (m a.s.l.)	Length (m)	Width (m)	Height (m)	Max Sample thickness (cm)	SUERC AMS ID (^{10}Be)	^{10}Be at/g Qtz	SUERC AMS ID (^{26}Al)	^{26}Al at/g Qtz	SUERC AMS ID (^{36}Cl)	^{36}Cl at/g rock
JRI 01	22/01/2011	N	Granite	104	1.62	1.28	0.3	3	b5325	76081 ± 2720	a1514	547648 ± 40912	-	-
JRI 03	22/01/2011	N	Granite	103	1.36	1.23	0.63	2	b5326	66821 ± 2759	a1515	564669 ± 28952	-	-
JRI 09	23/01/2011	N	Granite	39	3.6	3.15	1.2	1	b5331	51771 ± 1852	a1519	374483 ± 12691	-	-
JRI 26	29/01/2011	N	Granite	170	1.9	1.3	0.3	1	b5332	43227 ± 2337	a1536	347123 ± 22320	-	-
JRI 29	30/01/2011	N	Granite	25	2.1	1.4	1	2	b5346	35897 ± 2099	a1529	242612 ±28338	-	-
JRI 33	04/02/2011	N	Basalt	312	1.4	1.2	1	4	-	-	-	-	c2664	213916 ± 76286
JRI 34	04/02/2011	N	Basalt	244	1.7	1.3	0.7	1	-	-	-	-	c2665	258360 ± 75191
JRI 35	06/02/2011	N	Granite	45	3.4	2.1	0.6	1	b5333	36124 ± 1505	a1520	283267 ± 14631	-	-
JRI 49	11/02/2011	N	Granite	360	1.55	0.9	0.55	1	b5348	147849 ± 7181	a1532	897051 ± 121146	-	-
JRI 50	11/02/2011	N	Granite	370	1.55	1.1	0.75	1	b5349	116577 ± 5140	a1533	911094 ± 33796	-	-
JRI 62	20/02/2011	N	Granite	144	0.9	0.65	0.45	1	b5529	47779 ± 1938	a1600	414063±26819	-	-

Table 1

Sample	Elevation (m a.s.l.)	GPS (S)	GPS (W)	Location and context	^{10}Be age	^{26}Al age	^{26}Al/^{10}Be	^{36}Cl age	Considered Age
JRI01	104	63.84267	58.03217	San Carlos Hill; indicates age of incursion of APIS onto NW shore of JRI	12117 ± 435	12873 ± 968	7.2 ± 0.6	-	12244 ± 397
JRI03	103	63.84306	58.03126	San Carlos Hill; indicates age of incursion of APIS onto NW shore of JRI	10566 ± 437	13186 ± 680	8.5 ± 0.6	-	11332 ± 368
JRI09	39	63.85701	58.07312	Sharp Valley; indicates age of incursion of APIS onto NW shore of JRI	8637 ± 312	9264 ± 315	7.2 ± 0.4	-	8948 ± 222
JRI26	170	63.90809	57.89289	San Jose Pass; indicates exposure of interior of JRI	6321 ± 342	7486 ± 483	8.0 ± 0.7	-	6710 ± 279
JRI29	25	63.93596	57.81215	St. Martha Cove; indicates withdrawal of ice from eastern coast of JRI	6159 ± 361	6083 ± 713	6.8 ± 0.9	-	6143 ± 322
JRI33	312	63.90371	58.02856	Large basaltic boulder on drift sheet below Davies Dome; indicates exposure of interior of JRI	-	-	-	19929 ± 7285	19929 ± 7285
JRI34	244	63.90198	58.02380	Large basaltic boulder on drift sheet below Davies Dome; indicates exposure of interior of JRI	-	-	-	22114 ± 6614	22114 ± 6614
JRI35	45	63.80006	57.81549	Cape Lachmann; indicates incursion of APIS ice onto Cape Lachmann. Excluded as it is the youngest boulder in a case of geological scatter	6019 ± 251	6955 ± 360	7.8 ± 0.5	-	6325 ± 206
JRI49	360	63.83208	57.87360	Summit of Lachmann Mesa; indicates age of thick APIS over-riding JRI	17951 ± 876	16096 ± 2191	6.1 ± 0.9	-	17695 ± 813
JRI50	370	63.83592	57.87108	Summit of Lachmann Mesa; indicates age of thick APIS over-riding JRI. Excluded as it is the youngest boulder in a case of geological scatter	14004 ± 620	16192 ± 605	7.0 ± 0.5	-	15125 ± 433
JRI62	144	63.85960	58.10838	Stonely Point-Kaa Bluff; indicates age of incursion of APIS onto NW shore of JRI	7178 ± 292	9178 ± 597	8.7 ± 0.7	-	7564 ± 262

Table 2

Sample	NZ ^{10}Be	NZ ^{26}Al	Global ^{10}Be	Global ^{26}Al
JRI01	14099	14968	12117	12873
JRI03	12293	15332	10566	13186
JRI09	10105	10766	8687	9264
JRI26	7355	8703	6321	7486
JRI29	7107	7067	6159	6083
JRI35	7000	8081	6019	6955
JRI49	20909	18739	17951	16096
JRI50	16309	18851	14004	16192
JRI62	8351	10670	7178	9178

Table 3

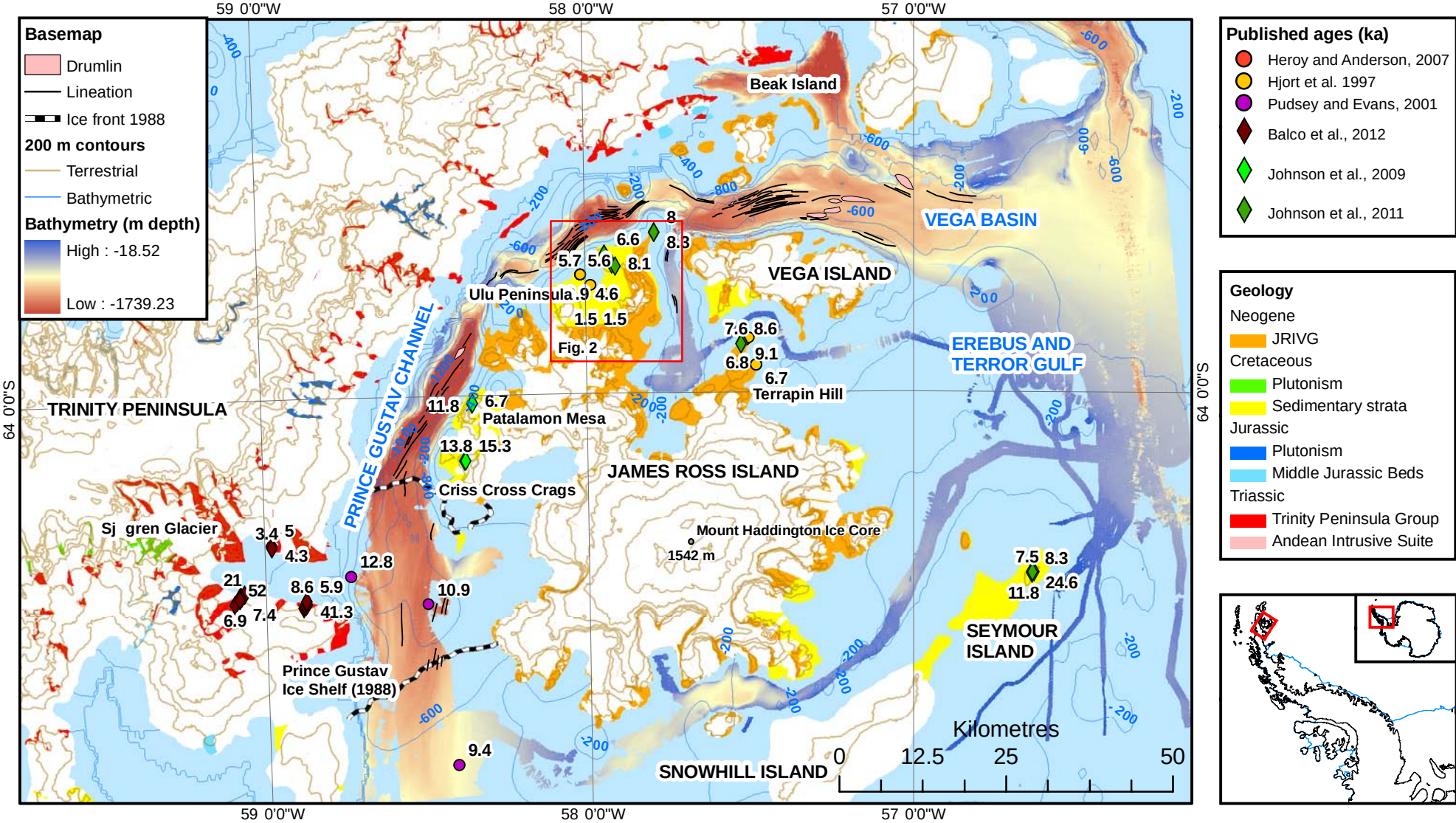
Basemap
Drumlin
Lineation
Ice front 1988
200 m contours
Terrestrial
Bathymetric
Bathymetry (m depth)
High : -18.52
Low : -1739.23
Published ages (ka)
Heroy and Anderson, 2007
Hjort et al. 1997
Pudsey and Evans, 2001
Balco et al., 2012
Johnson et al., 2009
Johnson et al., 2011
Geology
Neogene
JRIVG
Cretaceous
Plutonism
Sedimentary strata
Jurassic
Plutonism
Middle Jurassic Beds
Triassic
Trinity Peninsula Group
Andean Intrusive Suite
59 0'0"W
58 0'0"W
57 0'0"W
64 0'0"S
Beak Island
VEGA BASIN
VEGA ISLAND
EREBUS AND TERROR GULF
TRINITY PENINSULA
PRINCE GUSTAV CHANNEL
JAMES ROSS ISLAND
SEYMOUR ISLAND
SNOWHILL ISLAND
Ulu Peninsula
Fig. 2
Patalamon Mesa
Terrapin Hill
Criss Cross Crags
Sj gren Glacier
Mount Haddington Ice Core
1542 m
Prince Gustav Ice Shelf (1988)
Kilometres
0
12.5
25
50

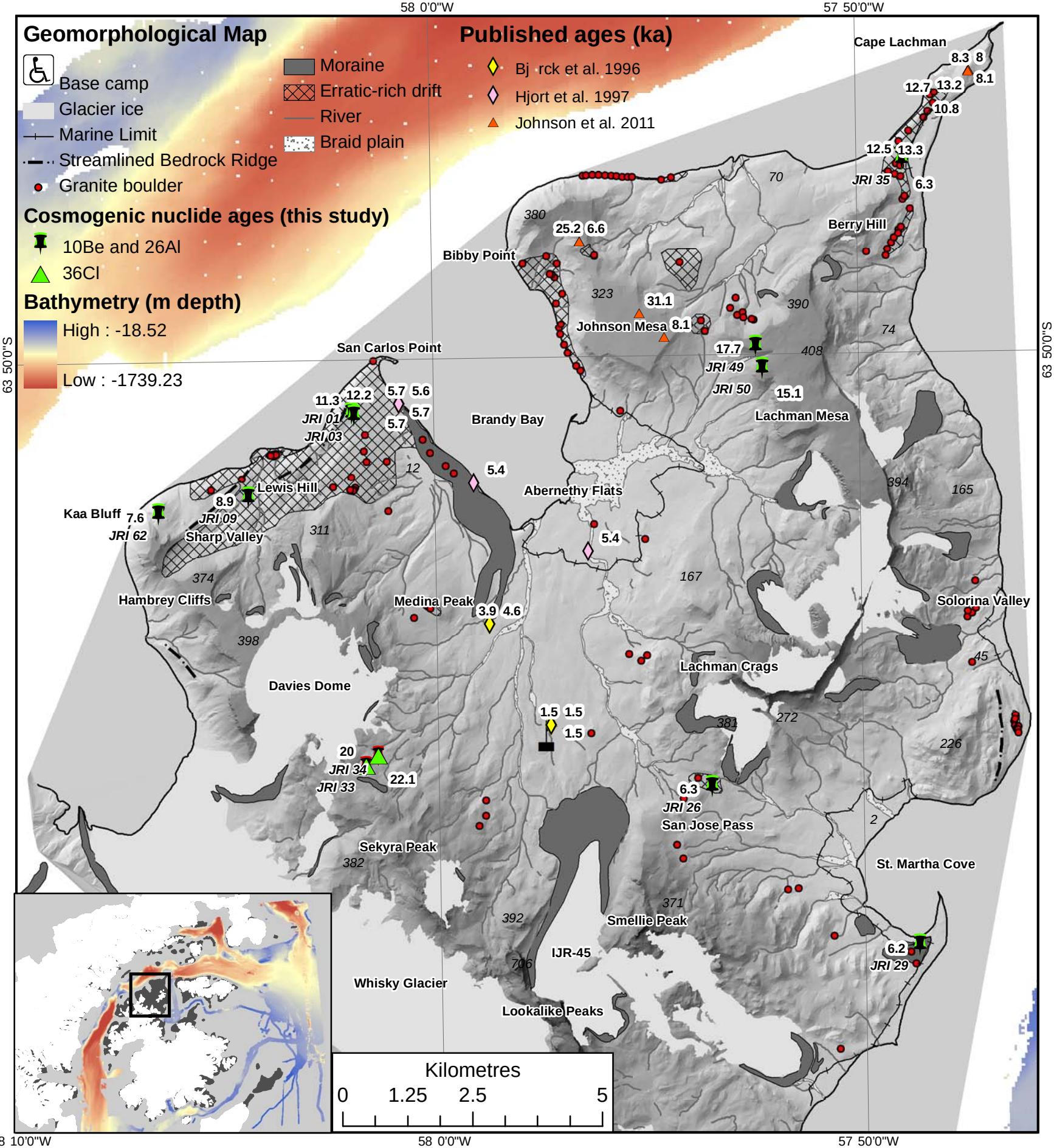
Geomorphological Map
Base camp
Glacier ice
Marine Limit
Streamlined Bedrock Ridge
Granite boulder
Moraine
Erratic-rich drift
River
Braid plain
Published ages (ka)
Bj rck et al. 1996
Hjort et al. 1997
Johnson et al. 2011
Cosmogenic nuclide ages (this study)
10Be and 26Al
36Cl
Bathymetry (m depth)
High : -18.52
Low : -1739.23
58 0'0"W
57 50'0"W
63 50'0"S
Cape Lachman
8.3
8
8.1
12.7
13.2
10.8
12.5
13.3
JRI 35
6.3
70
380
25.2
6.6
Berry Hill
Bibby Point
323
31.1
390
Johnson Mesa
8.1
74
San Carlos Point
17.7
408
JRI 49
JRI 50
15.1
11.3
12.2
5.7
5.6
JRI 01
5.7
Brandy Bay
Lachman Mesa
JRI 03
5.7
12
5.4
Lewis Hill
Abernethy Flats
394
165
Kaa Bluff
7.6
8.9
JRI 09
JRI 62
Sharp Valley
311
5.4
374
167
Hambrey Cliffs
Medina Peak
3.9
4.6
Solorina Valley
398
45
Lachman Crags
Davies Dome
1.5
1.5
1.5
381
272
226
20
JRI 34
JRI 33
22.1
6.3
JRI 26
San Jose Pass
2
Sekyra Peak
382
St. Martha Cove
371
392
Smellie Peak
IJR-45
6.2
JRI 29
706
Whisky Glacier
Lookalike Peaks
Kilometres
0
1.25
2.5
5


A

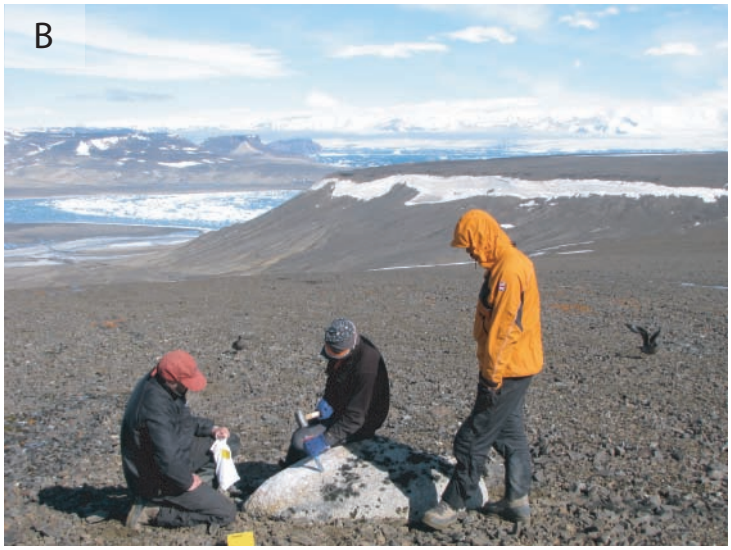
B


C


D

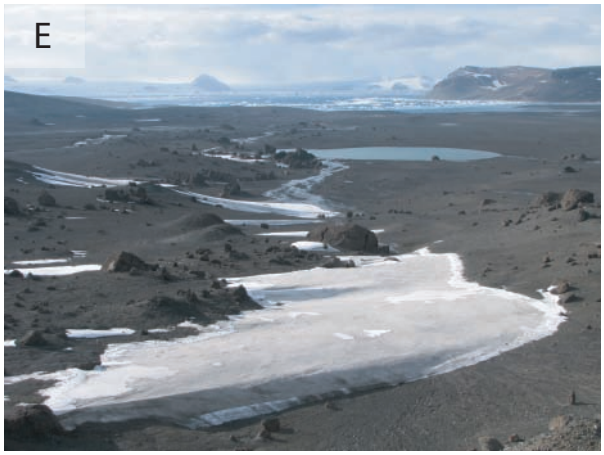
E

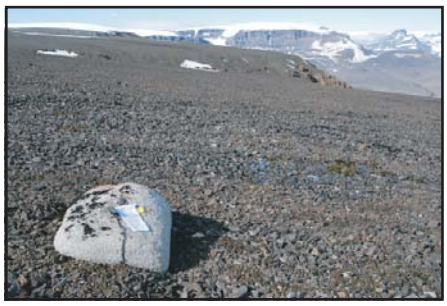

Sample: JRI 49 Lithology: Granite
Altitude: 360 m Age: 17.7 ± 0.8
Context: Lachman Mesa on hyaloclastite blockfield.

Sample: JRI 50 Lithology: Granite
Altitude: 370 m Age: 15.1 ± 0.4
Context: Lachman Mesa on hyaloclastite blockfield.

Sample: JRI 33 Lithology: Basalt
Altitude: 312 m Age: 19.9 ± 7.3
Context: Near Davies Dome. Basalt-rich drift.

Sample: JRI 34 Lithology: Basalt
Altitude: 244 m Age: 22.1 ± 6.6
Context: Near Davies Dome. Basalt-rich drift.

Sample: JRI 26 Lithology: Granite
Altitude: 170 m Age: 6.7 ± 0.3
Context: San Jose pass. Interior ice sheet.

Sample: JRI 29 Lithology: Granite
Altitude: 25 m Age: 6.1 ± 0.3
Context: St. Martha Cove. LGM moraine fragment. Interior ice sheet.

Sample: JRI 01 Lithology: Granite
Altitude: 104 m Age: 12.2 ± 0.4
Context: San Carlos Hill. Coastal erratic-rich drift.

Sample: JRI 03 Lithology: Granite
Altitude: 103 m Age: 11.3 ± 0.4
Context: San Carlos Hill. Coastal erratic-rich drift.

Sample: JRI 09 Lithology: Granite
Altitude: 39 m Age: 8.9 ± 0.2
Context: Sharp Valley. Coastal erratic-rich drift.

Sample: JRI 35 Lithology: Granite
Altitude: 45 m Age: 6.3 ± 0.2
Context: Cape Lachman. Coastal erratic-rich drift.

Sample: JRI 62 Lithology: Granite
Altitude: 144 m Age: 7.6 ± 0.3
Context: LGM moraine fragment on erratic-rich drift, Kaa Bluff. Coastal erratic-rich drift.

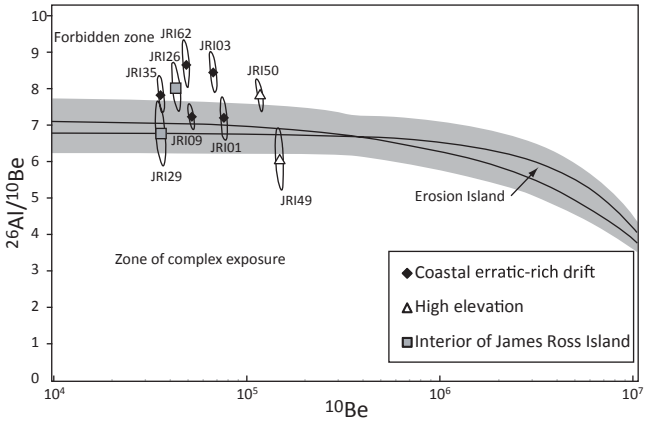
Forbidden zone
JRI62
JRI03
JRI26
JRI35
JRI50
JRI09
JRI01
JRI29
JRI49
Erosion Island
Zone of complex exposure
Coastal erratic-rich drift
High elevation
Interior of James Ross Island
$^{26}Al/^{10}Be$
^{10}Be
0
1
2
3
4
5
6
7
8
9
10
10^4
10^5
10^6
10^7

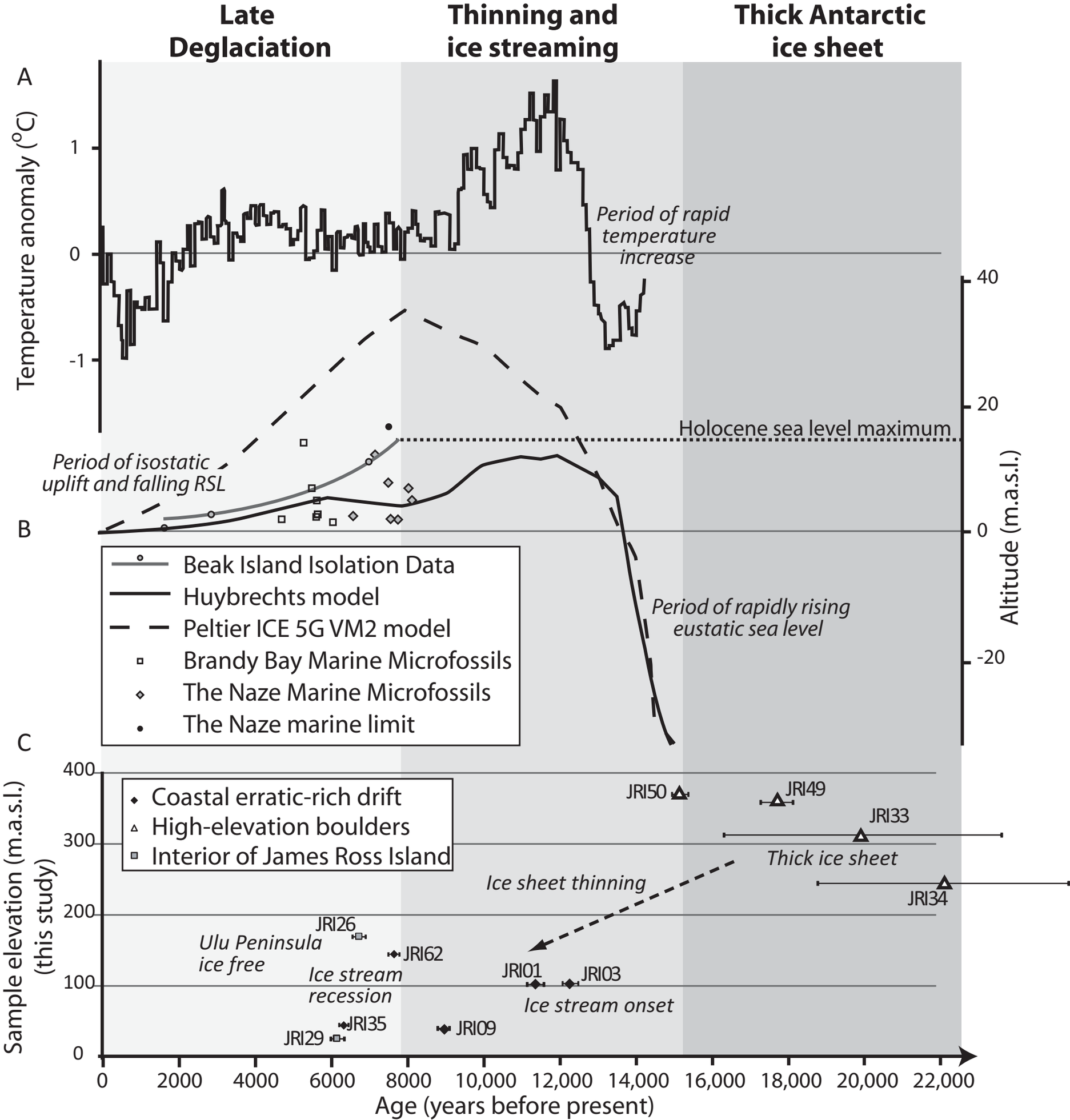
Late Deglaciation
Thinning and ice streaming
Thick Antarctic ice sheet
A
Temperature anomaly (°C)
1
0
-1
Period of rapid temperature increase
40
20
0
-20
Altitude (m.a.s.l.)
Holocene sea level maximum
Period of isostatic uplift and falling RSL
B
Beak Island Isolation Data
Huybrechts model
Peltier ICE 5G VM2 model
Brandy Bay Marine Microfossils
The Naze Marine Microfossils
The Naze marine limit
Period of rapidly rising eustatic sea level
C
Coastal erratic-rich drift
High-elevation boulders
Interior of James Ross Island
Sample elevation (m.a.s.l.) (this study)
400
300
200
100
0
JRI50
JRI49
JRI33
JRI34
Thick ice sheet
Ice sheet thinning
JRI26
JRI62
Ulu Peninsula ice free
Ice stream recession
JRI01
JRI03
Ice stream onset
JRI35
JRI29
JRI09
0
2000
4000
6000
8000
10,000
12,000
14,000
16,000
18,000
20,000
22,000
Age (years before present)